Characterization of compatible TRM composites for strengthening of earthen materials

Rui A. Silva, Daniel V. Oliveira, Cristina Barroso & Paulo B. Lourenço
ISISE & IB-S, University of Minho, Guimarães, Portugal, ruisilva@civil.uminho.pt

ABSTRACT: The high seismic vulnerability of earth constructions has been evidenced by several recent earthquakes that occurred around the World with moderate to high magnitudes, namely Bam 2003, Pisco 2007 and Maule 2010. The seismic risk associated to earth constructions is further amplified by the fact that a great percentage of these constructions is built on regions with important seismic hazard. Thus, the preservation of the immense earthen built heritage and of the life of their inhabitants demands adopting innovative strengthening interventions. However, the success of such solutions requires fulfilling compatibility requirements, while its general use requires adopting affordable materials and low complexity technical solutions. In the last years, textile reinforced mortars (TRM) have been increasingly used to strengthen masonry structures due to their high structural effectiveness and compatibility. In the case of earth constructions, these composite materials are also expected to provide efficient strengthening, though specific component materials should be adopted. This paper presents an experimental program dedicated to the characterization of the composite behavior of two TRM composites proposed for strengthening rammed earth walls. The composites differ on the mesh used, namely a low cost glass fiber mesh and a nylon mesh acquired locally, while the same earth-based mortar was used in both cases. The experimental program involved testing the mortar under compression and composite coupons under tension. In general, the glass TRM presents higher strength and stiffness in tension, while the nylon TRM presents considerably higher deformation capacity. Finally, stress-strain relationships describing the composite behavior are presented for numerical modelling purposes.

KEY WORDS: Earthen walls, strengthening, textile reinforced mortars, compatibility, low cost

1 Introduction

The high seismic vulnerability of earth constructions has been evidenced by recent earthquakes that occurred around the World with moderate to high magnitudes, namely Bam 2003, Pisco 2007 and Maule 2010. This vulnerability is a consequence of several factors (Yamín Lacouture et al., 2007 and Oliveira et al., 2010), among which the poor connections between structural elements, high self-weight and low mechanical properties are systematically the most emphasized ones. The seismic risk associated to earth constructions is further amplified by the fact that a great percentage of these constructions is built on regions with important seismic hazard.

Despite the current marginal use of rammed

earth in Portugal, the southern region of the country presents a significant built heritage, whose monolithic walls were erected by compacting moistened earth inside a formwork. Most of this heritage is concentrated in the Alentejo region (Rocha, 2005) and is mainly constituted by still inhabited dwellings. Nevertheless, this region is also characterized by a moderate seismic hazard, where the reference peak ground acceleration can achieve up to 2.0 m/s^2 according to Eurocode 8 (IPQ, 2009). This situation combined with the fact that earth constructions present high seismic vulnerability raise seismic risk concerns. The preservation of the immense earthen built heritage and of the life of their inhabitants demands adopting innovative strengthening interventions.

Textile reinforced mortar (TRM), also known as fiber reinforced cementitious matrix (FRCM), is an innovative strengthening solution that is becoming increasingly used for masonry structures. TRM is an externally bonded composite system composed of two material components, namely the matrix (mortar) and one or more layers of textile (fibers-meshes). The textile provides tensile strength to the system, while the embedding mortar provides protection against external agents and tensile stress transfer capacity between the support masonry and the textile. In general, the available commercial systems use high performance cement- or hydraulic lime-based mortars and meshes made of high tensile strength fibers, such as carbon, basalt and glass (De Felice et al., 2014). Recent research has been demonstrated that TRM strengthening allows to increase greatly the out-of-plane strength and deformation capacities of masonry walls (Valluzzi et al., 2014).

The success of TRM strengthening requires fulfilling compatibility requirements, while its general use requires adopting affordable materials and low complexity technical solutions. These aspects are particularly decisive in the strengthening of earthen walls. In this regard, the Pontifical Catholic University of Peru (PUCP) has been studying a solution, called geomesh strengthening, to strengthen adobe dwellings (Blondet et al., 2005), whose main outcomes resulted in design guidelines included in the Peruvian code E.080 (MVCS, 2017). This solution fits within the concept of TRM strengthening, as it includes the application of a low cost geosynthetic mesh tightly fixed to the adobe walls, covered by a coating mortar. The study of this technique has been mainly addressed by means of large-scale structural tests (Noguez & Navarro, 2005, Zavala & Igarashi, 2005, Figueiredo et al., 2013), which shown that the technique promotes a significant improvement of the seismic performance of adobe constructions. Nevertheless, the characterization of the strengthening solution is rarely addressed, namely with respect to the composite mechanical behavior and interaction between the different materials composing the solution, which define the efficiency of the strengthening (Kouris & Triantafillou, 2018).

The strengthening of rammed earth walls with TRM was recently proposed in Oliveira et al. (2017). This work investigated different low cost meshes readily available in the local market, which led to name the strengthening technique as low cost textile reinforced mortar (LC-TRM). Different coating mortars were also characterized in this study.

The experimental work presented in this paper is a sequence of the previously referred work, by investigating the composite behavior of two LC-TRM composites selected to be compatible with rammed earth. The composites differ on the mesh used, namely a low cost glass fiber mesh and a nylon mesh, while the coating mortar consists of an earth-based mortar.

2 Experimental program

The experimental program was carried out with the main objective of characterizing the composite behavior of two LC-TRM

composites selected to be compatible with rammed earth from Alentejo region, Portugal. This section presents the materials composing both composites and the experimental procedures followed to characterize the composite behavior.

2.1 Materials

The two adopted LC-TRM composites were composed with the same earth-based mortar and two different reinforcing meshes.

The composition of the earth-based mortar was defined previously in Oliveira et al. (2017), as mortar EM2.0. The mortar is constituted by 33% of sieved soil and 67% of quarzitic fine sand (0/2). The soil was collected from the municipality of Odemira, which is located in Alentejo region. This soil was previously used to manufacture representative rammed earth specimens (Silva et al., 2018) and was deemed as presenting very high clay content. The soil incorporated in the mortar was sieved to remove the particles larger than 10 mm, which corresponds to the recommended maximum particle size for earth-based mortars (Röhlen & Ziegert, 2011). The particle size distribution curves of the mortar and composing materials are given in Figure 1. The water solids ratio (W/S) was defined as 0.17, in order to obtain a flow table value (CEN, 2004) of about 170 m, as recommended in Gomes (2013). The mortar presented a linear shrinkage value of 0.7%, which is inferior to the recommended maximum value of 2% (Gomes, 2013). With respect to the physical-mechanical properties (CEN, 1999), the mortar presented a density of 1810 kg/m^3, flexural strength of 0.5 MPa and compressive strength of 0.9 MPa (equilibrium moisture content of 1.1% at 20ºC temperature and 57.5% relative humidity).

The meshes incorporated in the LC-TRM composites consisted of a woven glass fiber mesh (RM1) and a nylon mesh (RM2) with welded knots, as illustrated in Figure 2. Mesh RM1 was acquired with a cost of 0.85 €/m^2, presents a mesh aperture of 8x9 mm^2 and mass per unit area of 93 g/m^2, while those of mesh RM2 are 0.63 €/m^2, 16x21 mm^2 and 63 g/m^2, respectively. The tensile strength of both meshes is different in their main directions. In RM1 case, the tensile strength is 17 kN/m in the longitudinal (X) direction and 12 kN/m in the transversal (Y) one. The mesh RM2 is substantially weaker, as the tensile strength values are 2 kN/m and 4 kN/m, respectively. It should be noted that a nylon mesh similar to RM2 was previously used in the study presented in Figueiredo et al. (2013) to strengthen an adobe wall, while mesh RM1 was used in the study presented in Sadeghi et al. (2017) to strengthen adobe vaults.

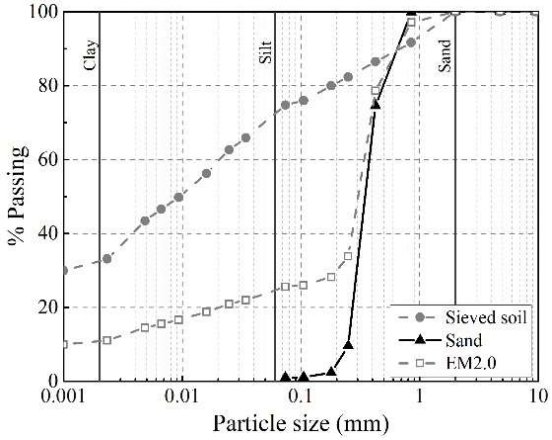

Figure 1. Particle size distribution of the mortar and composing materials.

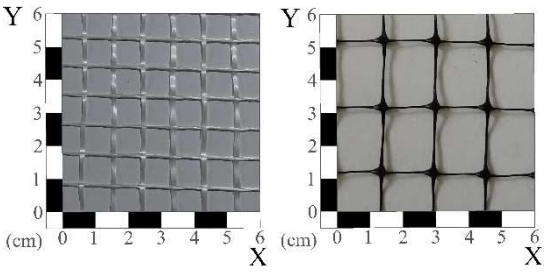

Figure 2. Reinforcing meshes adopted in the LC-TRM composites: (a) RM1; (b) RM2.

2.2 Testing methods

The composite behavior of both LC-TRM

composites was evaluated by testing individually the compressive behavior of the mortar and the tensile behavior of mortar-mesh coupons.

Three cylindrical specimens with 90 mm diameter and 180 mm height were prepared from the earth-based mortar EM2.0. This geometry results in a 2:1 height-diameter ratio, which mitigates the influence of the confinement introduced by the testing plates on the compression behavior. The specimens were casted in PVC molds, which were perforated with 1-2 mm holes spaced each 10 mm to promote the uniform drying hardening of the mortar inside the mold. This procedure allowed to demold the specimens after 7 days of drying in a climatic chamber at constant temperature of 20ºC and relative humidity of 57.5%. Then, the specimens were kept in the same climatic chamber to achieve equilibrium moisture content until testing, which occurred 28 days after casting. The tests were performed using a frame equipped with an actuator, which loaded the specimens under displacement control at constant speed of 3 μm/s. The axial deformation at the middle third of the specimens was monitored by means of three linear variable differential transducers (LVDTs) fixed with aluminum rings. The test setup is illustrated in Figure 3a.

Four coupon specimens were prepared for each LC-TRM composite in order to test their tensile behavior. The specimens consisted of mortar bands with one embedded layer of mesh positioned at middle thickness. They were casted by placing in a mold a mortar layer with dimensions 300 mm length, 60 mm width and 5 mm thickness. Then, a layer of mesh was placed covering the mortar by slightly stretching it. The mesh layer was longer than the mortar one so that the excess extremities presented a length of 50 mm to bond the gripping steel plates before testing. It should be noted that only the direction of the highest tensile strength of each mesh was considered for testing the composite behavior, meaning that the mesh layers in the coupons were orientated accordingly. A second layer of mortar with the same dimension of the first was applied subsequently. The specimens were stored until testing in the same ambient conditions of the previously referred climatic chamber. Demolding was also performed 7 days after casting. The tensile tests were performed at 28 days of age by adopting a procedure similar to that of ASTM D6637 (ASTM, 2011). Gripping plates were glued to the excess mesh extremities with an epoxy mortar one day before testing. Then, the specimens were fixed to the grips of the testing machine and the tensile load was applied under displacement control (see Figure 3b). Due to the remarkable difference in stiffness between both meshes, different testing speed protocols were used for each case. For RM1 coupons, a constant speed of 3 μm/s was applied until an axial deformation of 2 mm was reached, after which the speed was increased to 10 μm/s until failure. RM2 coupons were loaded with 30 μm/s of speed until an axial a deformation of 6 mm was obtained and then at 100 μm/s. The axial deformation was monitored by means of a LVDT fixed between the two grips fixing the coupons.

(a) (b)

Figure 3 . Testing setups of the LC-TRM composites: (a) compression test of the mortar; (b) tensile test of the coupons.

3 Results and discussion

The mortar cylinders tested under compression

presented an average density of 1876 kg/m^3 and equilibrium moisture content of 0.5%. The obtained stress-strain curves are presented in Figure 4. The average compressive strength is of about 1.3 MPa (CoV= 5%) and the Young's modulus is 3322 MPa (CoV= 13%), which was computed by linear fitting of the stress-strain curves at 5-30% of the compressive strength. The curves present an expressive nonlinear behavior, which is typically observed in earthen materials.

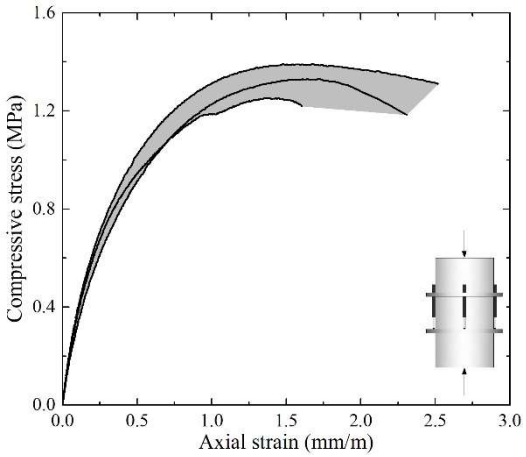

Figure 4. Stress-strain curves obtained from the compression tests on the mortar specimens.

The results of the tensile tests on the coupons of both reinforcing meshes are presented in Figure 5 in terms of stress-strain curves and typical failure modes. It should be noted that the tensile stress was computed by considering the cross section of the coupon, instead of the undetermined cross section of the reinforcing mesh. In average, the tensile strength of the RM1 coupons is of about 1.6 MPa (CoV= 6%), while that of the RM2 coupons is of about 0.4 MPa (CoV= 4%). As expected, the mesh RM1 provides higher strength to the LC-TRM composite than mesh RM2. Furthermore, both meshes when integrating the LC-TRM composite are able to achieve tensile strength values similar to those of the dry meshes. For comparison purposes, the average linear strength of the coupons RM1 and RM2 is of 16.4 kN/m and 4.3 kN/m, respectively. On the other hand mesh RM2 provides much higher deformation capacity than mesh RM1. This behavior results from the high flexibility and plastic behavior of mesh RM2 as discussed in Oliveira et al. (2017). Another consequence of this characteristic on the composite behavior seems to be the higher capacity to redistribute stresses, which is observed in terms of formation of higher number of cracks in RM2 coupons.

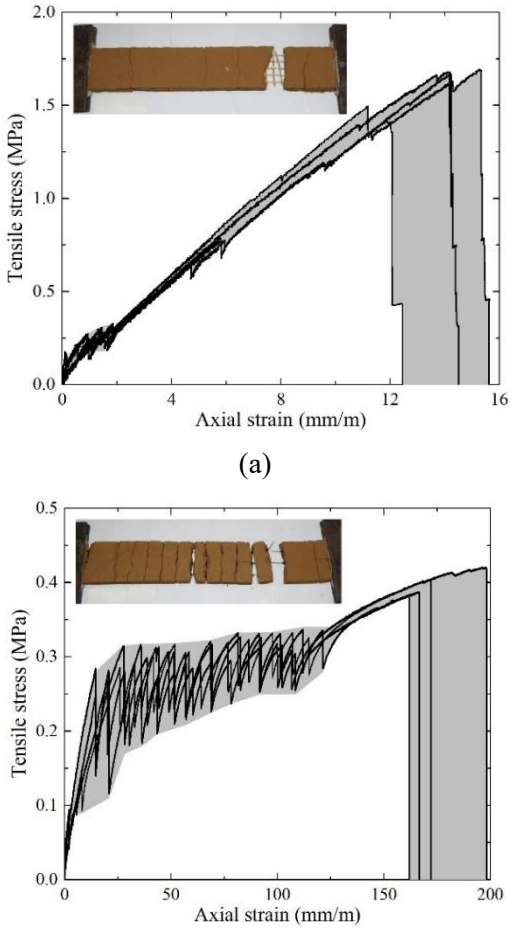

Figure 5. Stress-strain curves and failure modes obtained from the tensile tests: (a) RM1; (b) RM2.

The tensile behavior of both LC-TRM composites is in agreement with the typical behavior described in Ascione et al. (2015) for TRM composites. In this regard, three stages are depicted in the stress-strain curves. Stage I

corresponds to the uncracked behavior, stage II to the crack development and stage III to the cracked behavior. In stage I the response is linear, as the mortar is not cracked. Afterwards, the appearance of the first crack occurs and in stage II the stiffness of mortar is decreased with the development of further cracks. Thus, in these first two stages, the behavior of the composite depends on the mechanical properties of the mortar, mesh and on the interaction of these two components. After a certain strain level, the formation of new cracks stops and a slight increase in force is observed, which defines the transition to stage III. Here, the increase in tensile stress leads to the widening of the cracks, where the loading capacity of the system is defined by the mechanical properties of the mesh (textile).

The curves of Figure 6 summarize the results of the experimental program by proposing simplified curves that are expected to be used in future numerical modeling investigations.

As previously referred to, the compression behavior of the LC-TRM is defined by the individual behavior of the earth-based mortar. Furthermore, past research has demonstrated that the expressive nonlinear behavior of earthen materials in compression is better defined by a multilinear stress-strain relationship, which was here also adopted (Miccoli et al., 2019). The initial branch of the proposed relationship represents the linear behavior by means of the experimental Young's modulus up to stress value of 30% of the compressive strength (see Figure 6a). Then, it follows the average curve obtained from the experimental tests. This average is interrupted by an idealized post-peak linear degradation, defined with basis on the trend observed from the experimental curves. It should be noted that readings from the LVDTs loose coherence in the post-peak phase due to interference of the damage development.

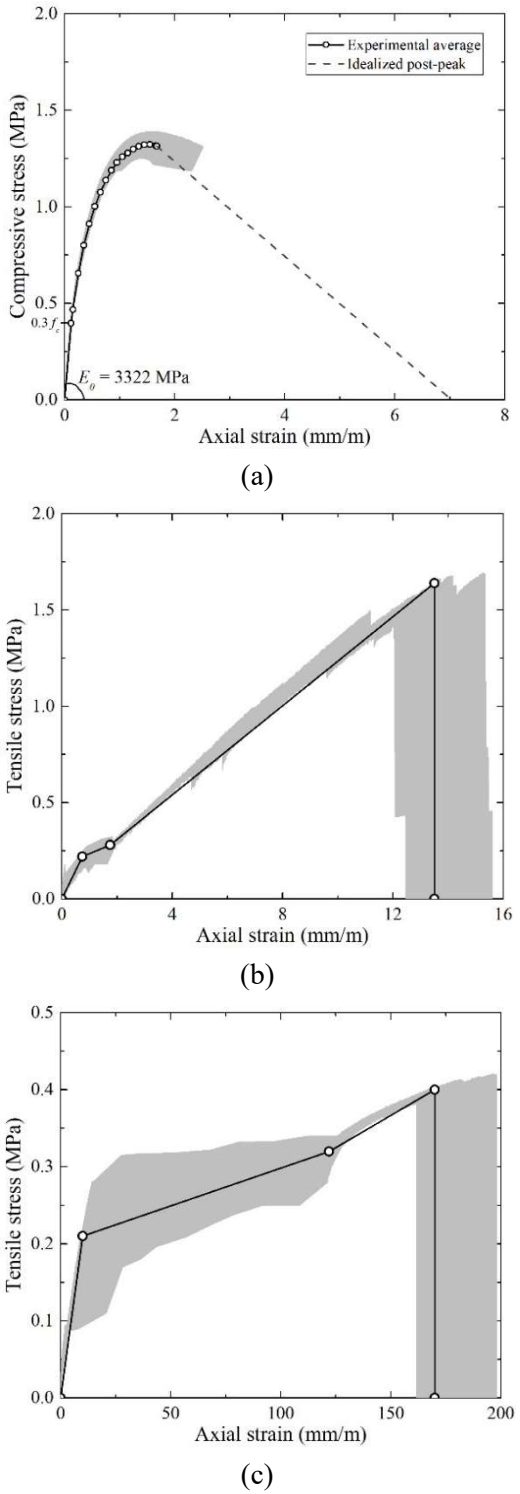

Figure 6 . Simplified curves of the LC-TRM composite behavior: (a) mortar in compression; (b) RM1 in tension; (c) RM2 in tension.

Regarding the tensile behavior of the LC-TRM composite, it was observed that it depends on the type of embedded mesh. Thus, a stress-strain relationship is here proposed for each mesh. In both cases, the relationship is a trilinear curve representing the three stages typically observed.

4 Conclusions

This paper presents an experimental program dedicated to the characterization of the composite behavior of two LC-TRM composites proposed for the strengthening of rammed earth walls. The composites differ on the mesh used, namely a low cost glass fiber mesh and a nylon mesh, while the coating mortar is the same and consists of an earth-based mortar. The composite behavior was characterized by testing the mortar under compression and composite coupons under direct tension.

The mortar presented an expressive nonlinear behavior typically observed in earthen materials. Despite that, the average values of the compressive strength and Young's modulus are 1.3 MPa and 3322 MPa, respectively.

In tension, the LC-TRM composite incorporating the glass fiber mesh (RM1) presents higher strength and stiffness than the composite incorporating the nylon mesh (RM2). On the other hand, the deformation capacity of the second is considerably higher. Furthermore, the typical three stages behavior of TRM was observed in both LC-TRM composites.

Finally, stress-strain relationships were proposed to simulate the composite behavior of both LC-TRM solutions in future numerical modelling investigations.

Acknowledgements

This work was partly financed by FEDER funds through the Competitivity Factors Operational Programme - COMPETE and by national funds through FCT – Foundation for Science and Technology within the scope of projects POCI-01-0145-FEDER-007633 and POCI-01-0145-FEDER-016737.

References

[1] Ascione, L., de Felice, G. & De Santis, S. 2015. A qualification method for externally bonded Fibre Reinforced Cementitious Matrix (FRCM) strengthening systems. Composites Part B: Engineering, 78: 497-506.

[2] ASTM. 2011. D6637-11: Standard Test Method for Determining Tensile Properties of Geogrids by the Single or Multi-Rib Tensile Method. West Conshohocken: ASTM International.

[3] Blondet, M., Torrealva, D., Garcia, G., Ginocchio, F. & Madueño, I. 2005. Using industrial materials for the construction of safe adobe houses in seismic areas. EarthBuild2005 International Conference, Sydney.

[4] CEN. 1999. EN 1015-11: Methods of test for mortar for masonry - Part 11: Determination of flexural and compressive strength of hardened mortar. Brussels: European Committee for Standardization.

[5] CEN. 2004. EN 1015-3: Methods of test for mortar for masonry - Part 3: Determination of consistence of fresh mortar (by flow table). Brussels: European Committee for Standardization.

[6] De Felice et al. 2014. Mortar-based systems for externally bonded strengthening of masonry. Materials and structures, 47(12): 2021-2037.

[7] Figueiredo, A., Varum, H., Costa, A. & Oliveira, C. 2013. Seismic retrofitting solution of an adobe masonry wall. Materials and Structures, 46(1): 203-219.

[8] Gomes, M.I. 2013. Conservation of rammed earth construction: repairing mortars. PhD thesis. Universidade Nova de Lisboa. (in Portuguese)

[9] IPQ. 2009. NP ENV 1998-1: Eurocode 8: Design of structures for earthquake resistance – Part 1: General rules, seismic actions and rules for buildings. Lisbon: Instituto Português

da Qualidade.
[10] Kouris, L.A.S. & Triantafillou, T.C. 2018. State-of-the-art on strengthening of masonry structures with textile reinforced mortar (TRM). Construction and Building Materials, 188: 1221-1233.
[11] MVCS. 2017. Norma E.080: Diseño y Construcción con Tierra Reforzada. Normas legales, Anexo – resolución ministerial nº 121-2017-vivienda, Ministerio de Vivienda, Construcción y Saneamento.
[12] Noguez, R. & Navarro, S. 2005. Reparación de muros de adobe com el uso de mallas sintéticas. PUCP, International Conference SismoAdobe2005. (in Spanish)
[13] Oliveira, D.V., Silva, R.A., Lourenço, P.B. & Schueremans, L. 2010. As construções em taipa e os sísmos. Congresso Nacional de Sismologia e Engenharia - SÍMICA 2010, Aveiro (in Portuguese)
[14] Oliveira, D.V., Silva, R.A., Barroso, C. & Lourenço, P.B. 2017. Characterization of a Compatible Low Cost Strengthening Solution Based on the TRM Technique for Rammed Earth. In Key Engineering Materials, 747: 150-157.
[15] Rocha, M. 2005. Rammed earth in traditional architecture: construction techniques. Earth Architecture in Portugal. Lisbon: Argumentum.
[16] Röhlen, U. & Ziegert C. 2011. Earth Building Practice. Planning, Design, Building. Berlin: Beuth Verlag.
[17] Sadeghi, N, Oliveira, D.V., Silva, R.A., Mendes, N., Correia, M. & Azizi-Bondarabadi H. 2017. Performance of adobe vaults strengthened with LC-TRM: an experimental approach. PROHITECH'17, Lisbon.
[18] Miccoli, L., Silva, R.A., Oliveira, D.V. & Müller, U. 2019. Static Behavior of Cob: Experimental Testing and Finite-Element Modeling. Journal of Materials in Civil Engineering, 31(4): 04019021.
[20] Silva, R.A., Domínguez-Martínez, O., Oliveira, D.V. & Pereira, E.B. 2018. Comparison of the performance of hydraulic lime-and clay-based grouts in the repair of rammed earth. Construction and Building Materials, 193: 384-394.
[21] Valluzzi, M.R., Da Porto, F., Garbin, E. & Panizza, M. 2014. Out-of-plane behaviour of infill masonry panels strengthened with composite materials. Materials and structures, 47(12): 2131-2145.
[22] Yamín Lacouture, L.E., Phillips Bernal, C., Ortiz, R., Carlos, J. & Ruiz Valencia, D. 2007 Estudios de vulnerabilidad sísmica, rehabilitación y refuerzo de casas en adobe y tapia pisada. Apuntes: Cultural-Journal of Cultural Heritage Studies 20(2): 286-303 (in Spanish)
[23] Zavala, C. & Igarashi, L. 2005. Propuesta de Reforzamiento para Muros de Adobe. . PUCP, International Conference SismoAdobe2005. (in Spanish)